



UNIVERSITY OF LEEDS

This is a repository copy of *Stability and photo-thermal conversion performance of binary nanofluids for solar absorption refrigeration systems*.

White Rose Research Online URL for this paper:
<http://eprints.whiterose.ac.uk/155120/>

Version: Accepted Version

Article:

Nourafkan, E orcid.org/0000-0002-1898-5528, Asachi, M, Jin, H et al. (2 more authors) (2019) Stability and photo-thermal conversion performance of binary nanofluids for solar absorption refrigeration systems. *Renewable Energy*, 140. pp. 264-273. ISSN 0960-1481

<https://doi.org/10.1016/j.renene.2019.01.081>

© 2019 Published by Elsevier Ltd. This manuscript version is made available under the CC-BY-NC-ND 4.0 license <http://creativecommons.org/licenses/by-nc-nd/4.0/>.

Reuse

This article is distributed under the terms of the Creative Commons Attribution-NonCommercial-NoDerivs (CC BY-NC-ND) licence. This licence only allows you to download this work and share it with others as long as you credit the authors, but you can't change the article in any way or use it commercially. More information and the full terms of the licence here: <https://creativecommons.org/licenses/>

Takedown

If you consider content in White Rose Research Online to be in breach of UK law, please notify us by emailing eprints@whiterose.ac.uk including the URL of the record and the reason for the withdrawal request.



eprints@whiterose.ac.uk
<https://eprints.whiterose.ac.uk/>

Stability and photo-thermal conversion performance of binary nanofluids for solar absorption refrigeration systems

School of Chemical and Process Engineering, University of Leeds, Leeds, LS2 9JT, United Kingdom

Abstract

The Stability and photo-thermal conversion characteristics of a novel binary iron oxide nanofluid (including 50 wt% lithium bromide and 50wt% water) were investigated in this work. The stability of the binary nanofluid against agglomeration and sedimentation was analyzed by a centrifuge analyzer and transmission and electron microscopy (TEM), and the effects of iron oxide nanoparticle concentration and morphology on photo thermal conversion efficiency of nanofluid using a solar simulator were studied. Highly stable nanofluids were formulated. Experimental results indicated that the use of binary nanofluid could significantly increase light trapping efficiency to increase the bulk temperature, and in the same time, increase the evaporation rate due to surface localized heat generation. Possessing both high stability and excellent photothermal conversion rate, iron oxide nanoparticle is suggested as a good candidate for using in solar absorption refrigeration systems.

Keywords: Binary nanofluid, lithium bromide, solar absorption refrigeration system, photo-thermal conversion,

1. Introduction

Utilizing solar light as a green energy to run air conditioning systems is a promising technique to replace conventional systems driven by electricity. Solar-driven absorption refrigeration technology has the potential to reduce the peak electricity demand and the global warming. A binary fluid, lithium bromide-water, is one of the common fluids that used for solar thermal air conditioning (Fig. 1a) [1, 2]. It is based on a vapor absorption refrigeration cycle, where water is used as the refrigerant while lithium bromide is used as the absorbent [1].

The concentration of LiBr salt differs from one design to another, falling into a large range of 10-50 weight percent in an absorption refrigeration system[3]. In addition, the concentration of LiBr salt is varied in different parts of solar adsorption refrigeration systems, e.g. the generator or the absorber [4].

It has been reported that by dispersing stable NPs, more solar light energy could be trapped that improve the system efficiency [5, 6], and an improved heat transfer process could be achieved. It is expected that the efficiency of solar air conditioner could be increased by using a lithium bromide based nanofluids. It has been suggested that with appropriate modification of the system, the added nanoparticle could improve the solar absorption, hence increasing the separation effect, and in the same time, improve the absorption efficiency [xx]. However a number of challenges need to be solved first, and one in the forefront is the stability issue. Though there are plenty of nanofluids and nanofluid stability work published, nearly all were based on a single base fluid, either water or oil. The stability of nanoparticle in a pure fluid is relatively easier to be achieved, however for a binary fluid, especially with a high ionic component such as lithium bromide, it is much more difficult. The high concentration of LiBr would compress the electrical double layer (EDL) around NPs (Fig. 1b). The combined magnetic and Van der Waals attractive forces would dominate the electrostatic repulsion, which results in the agglomeration of NPs. There are basically two possible approaches to achieve a good dispersion and stability of nanoparticles: particle morphology control and extra steric stabilization. Colloid chemistry suggested that when the size of particles in a fluid is smaller than a critical size, R_c , Brownian motion of nanoparticles (diffusion) would overcome the sedimentation to form a stable dispersion [9]. In addition, the decrease of electrostatic repulsion force arising from the compression of EDL could be compensated by an effective functionalizing of NPs that promote steric repulsion. In addition, the photothermal conversion characteristics of a binary nanofluid is barely studied, albeit a large number of publications have been reported for pure liquid [xx]. The mechanisms of evaporation and steam generation enabled by nanoparticles are still under debate [xxx].

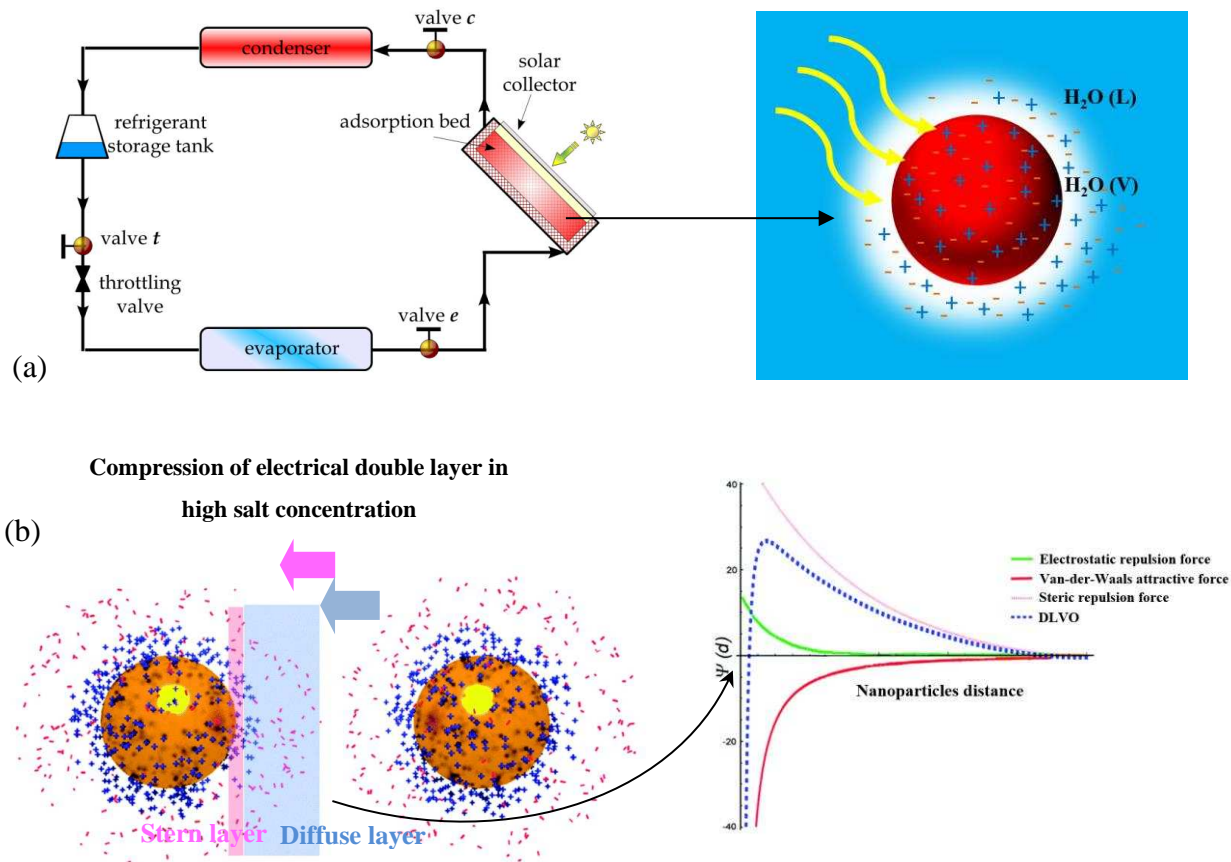


Fig. 1. (a) Solar-based applications such as solar thermal air conditioning (b) Compression of electrical double layer in high ionic media

Among various nanoparticle synthesis techniques, chemical precipitation reaction inside nanodroplets of a reverse microemulsion is a versatile method for synthesizing and functionalizing NPs simultaneously (Fig. 2) [10]. Some stabilizers in the structure of microemulsions could control the growth rate of different crystal facets of NPs, which leads to form different NPs morphologies (e.g. spheres, rods or disks) [11]. For example, Vidal-Vidal et al. [12] synthesized iron oxide NPs by using oleylamine and cyclohexylamine as precipitating agents, and showed the formed NPs were well crystallized, spherical shaped and capped with a monolayer coating of oleic acid, having a narrow size distribution of 3.5 ± 0.6 nm. In another study, Han et al., [13] synthesised iron oxide NPs using n-octane/water/CTAB/butanol microemulsion and obtained NPs with average size of 82.7, 51.4 to 27.2 nm by increasing the weight ratio of CTAB to n-octane from 0.25, 0.33 to 0.5 respectively.

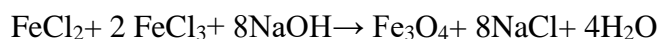
This work aims to develop a novel method of engineering stable nanoparticle dispersions into a binary fluid including high concentrations of lithium bromide, and investigate their photothermal conversion efficiencies. Iron oxide nanoparticle is selected as a low cost and promising NP in absorbing solar energy [7, 8], and synthesized via the reverse microemulsion method. Steric stabilization with careful selection of surfactants is used to form stable nanoparticle dispersions, whose performance is assessed by a centrifuge method via a LUMiSizer. The photo-thermal conversion and evaporation rate analysis of the engineered nanoparticle dispersions are investigated under a solar simulator.

2. Experiment

2.1. Material and Characterization

Analytical grade materials including cyclohexane, sorbitanmonooleate (Span 80, HLB=4.3), polyethylene glycol sorbitanmonolaurate (Tween 80, HLB=15), propyl alcohol, sodium hydroxide, ferric chloride (FeCl₃), ferrous chloride (FeCl₂), lithium bromide, citric acid were purchased from Sigma-Aldrich and used with no further processing.

Iron oxide NPs were synthesized inside the reverse microemulsion method using Massart co-precipitation reaction as follow [14]:



Our developed method by co-surfactants is used in this work [15] to produce stable reverse microemulsions. In the synthesis, different concentration of ferrous chloride (0.01, 0.05 and 0.1 molar) were used for NPs preparation at room temperature and 70 °C. The concentration of other reactants was prepared based on chemical stoichiometry with ferrous chloride. The sodium hydroxide solution as the reduction agent was added drop wise to the reverse microemulsion for a period of 10 min. The mixture was stirred over 4 h to reach the equilibrium. The phase

separation and phase transformation methods have been applied to produce final iron oxide nanofluids, which will be discussed in result section in more detail.

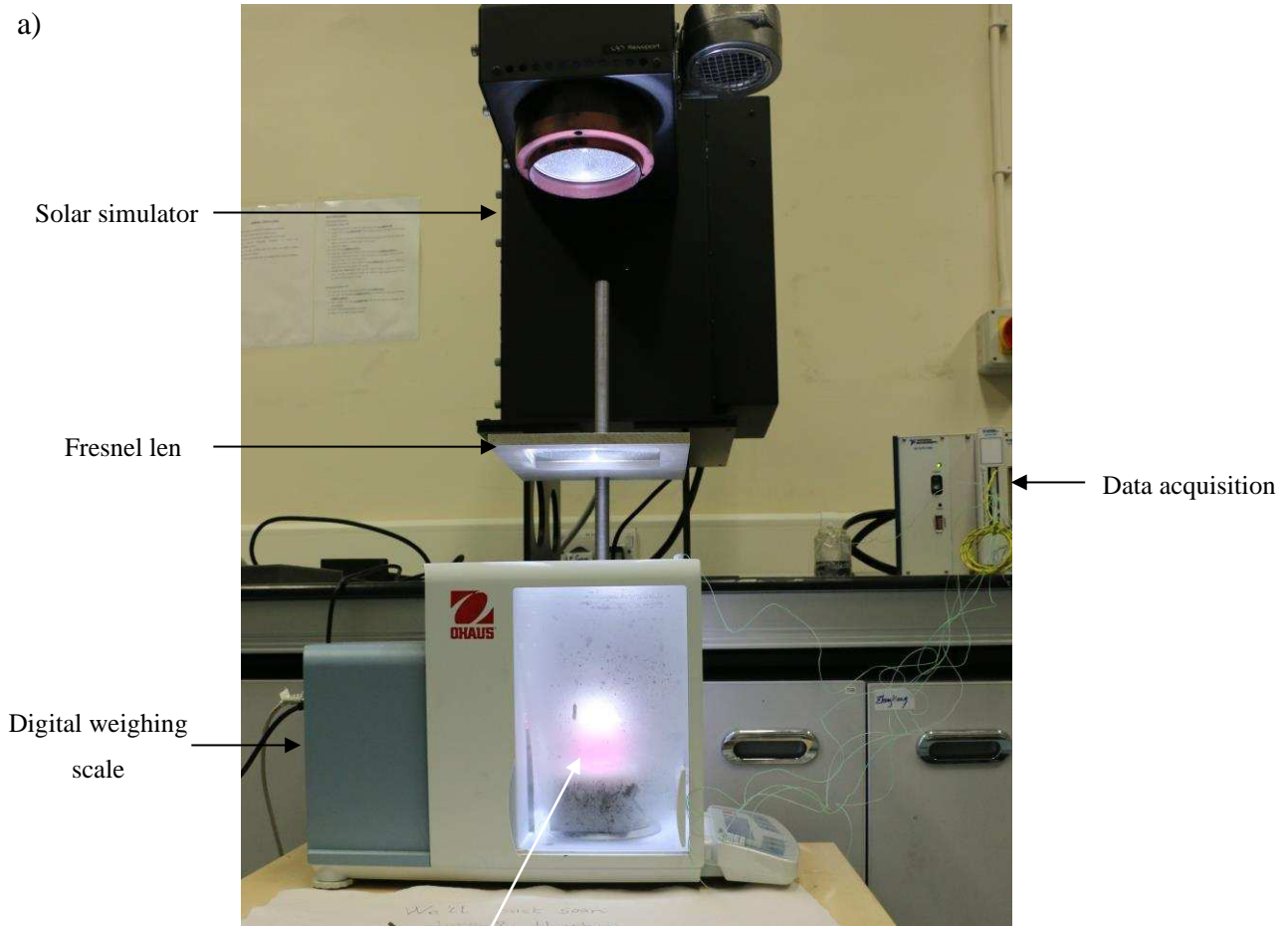
The formed NPs were analyzed by UV-spectrophotometer (Shimadzu, UV 1800), Transmission electron microscope (FEI Tecnai TF20 TEM), dynamic light scattering (Malvern Zetasizer ZS) and dispersion analyzer centrifuge (LUMiSizer, Lum GmbH, Berlin, Germany). Varian 240FS atomic absorption spectrophotometry (Varian Ltd, USA) was applied for the determination of iron oxide concentration.

2.2. Photo-thermal conversion evaluation

A ORIEL^R Sol3ATM Class AAA solar simulator (Newport) was used for photo-thermal conversion characteristics of nanoparticles in order to minimize the experimental uncertainties under direct sun light. This sun simulator provides a radiation spectrum matches the solar spectra, and the intensity can be varied by using suitable filters. This device is certified to IEC 60904-9 2007 edition, JIS C 8912 and ASTM E 927-05 standards.

In the experiments, (Fig. 3a), 10 cc iron oxide nanofluid was placed in the sample container (Fig. 3b) and a Fresnel lens (5 inches Diameter, eo^R Edmund optics) with a 30 cm focal distance was used to focus the sunlight. A digital weighing scale weighing scale with 4 digits (DV114C Ohaus) was used to measure evaporated mass change. In order to investigate the temperature distribution inside the sample, 8 K-type thermocouples (Omega TT-T-40-SLE) with a precision of $\pm 0.5^{\circ}\text{C}$ were used. Among which 6 thermocouples were put inside the solar receiver to measure the temperature gradient along the light pathway, one thermocouple was put

above the surface of testing sample, and another was used to measure the ambient temperature (Fig. 3c). A data acquisition system was used to record the readings from thermocouples and digital weighing scale. Before the experiment, the sample containers was washed carefully with pure water of ambient temperature, and all the samples were put inside a fridge and maintained the same starting temperature (20 °C). During the preparation stage, all nanofluids were avoided to expose sunlight.



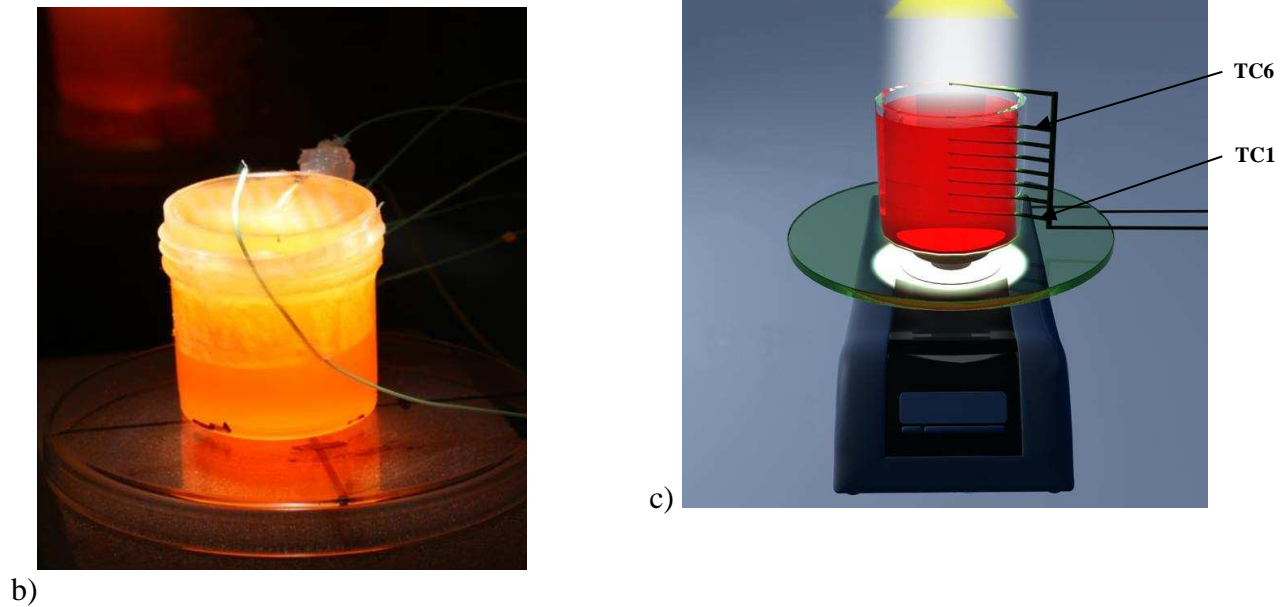


Fig. 3. a) Experimental set up of solar-driven evaporation, b) testing container containing binary nanofluid under 10 sun solar radiation and c) schematic place of thermocouples.

3. Results and Discussion

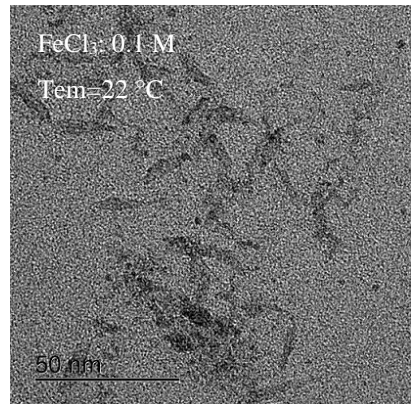
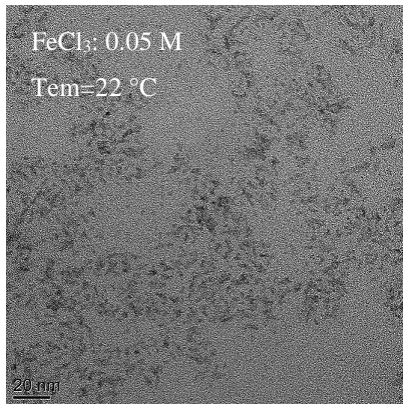
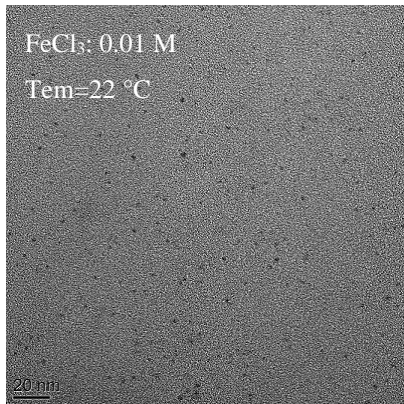
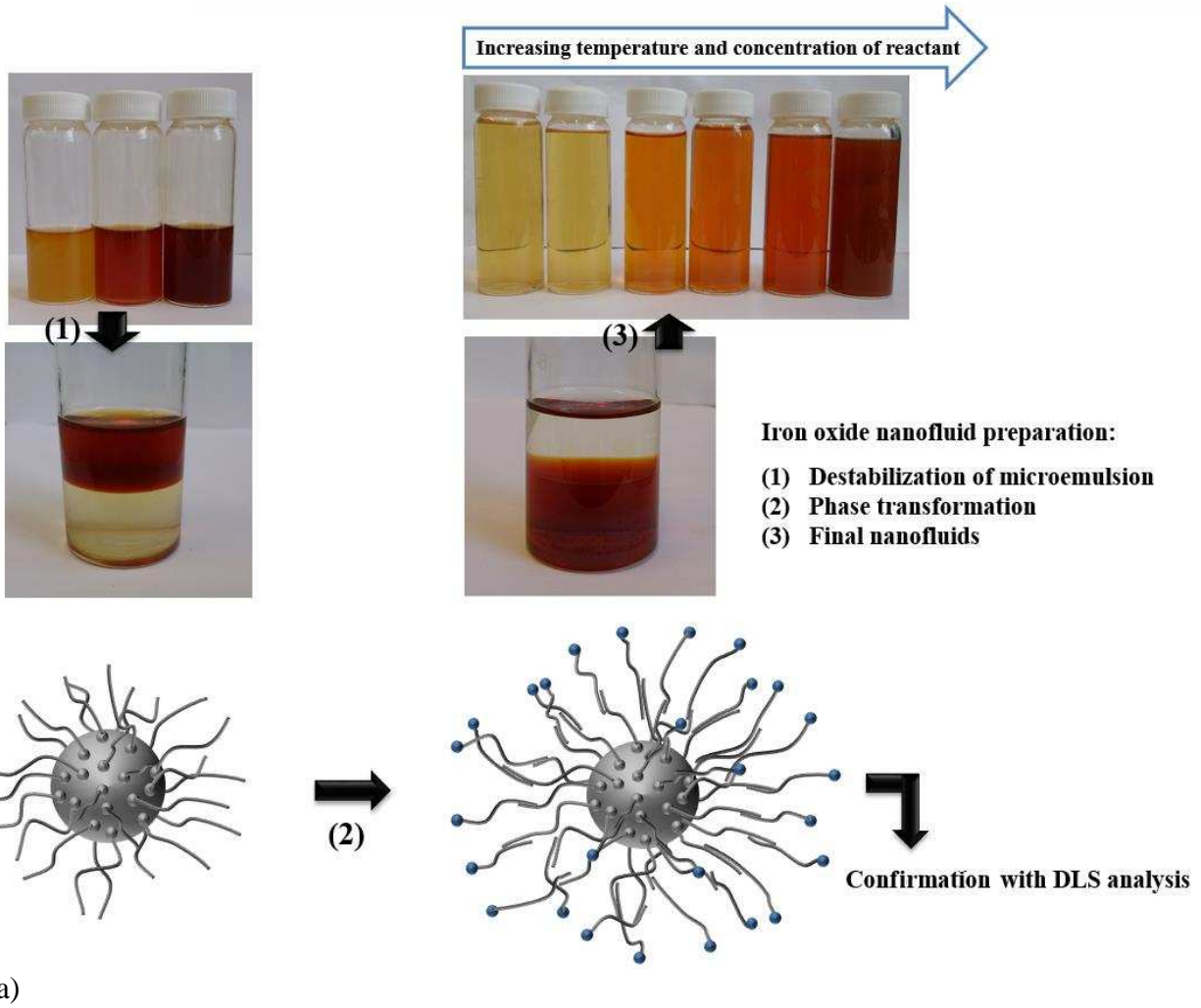
3.1. Binary nanofluid preparation and characterization

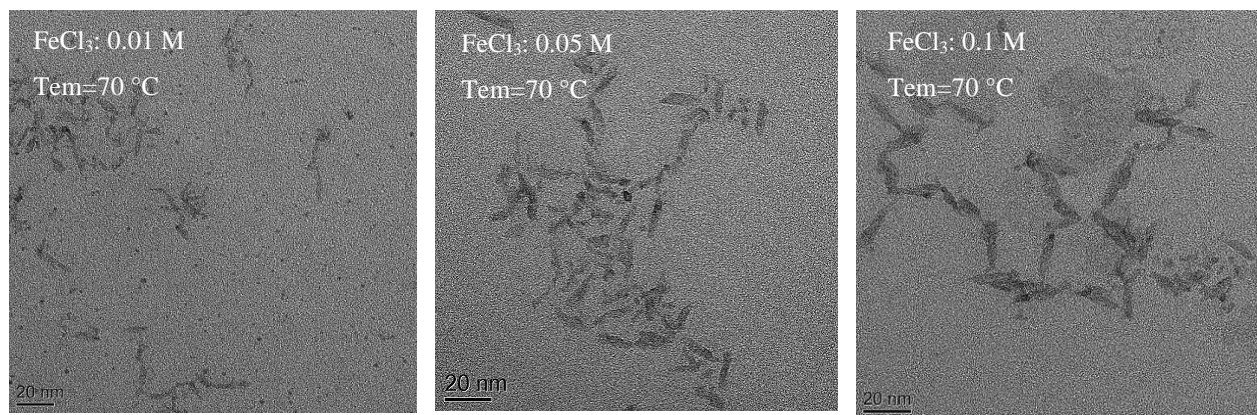
Fig. 4a illustrates the procedure of preparation and functionalizing of iron oxide NPs. The following steps have been applied after the formation of NPs inside reverse microemulsion:

- Organic and aqueous phase separation were done by destabilizing the reverse microemulsion via addition of extra pure water. In this stage, NPs remain inside the organic phase since the tails of stabilizer molecules are hydrophobic/oiliphilic. In fact, the NPs surface were covered with a single layer of stabilizer molecules so that the tail of stabilizers are free in organic phase.

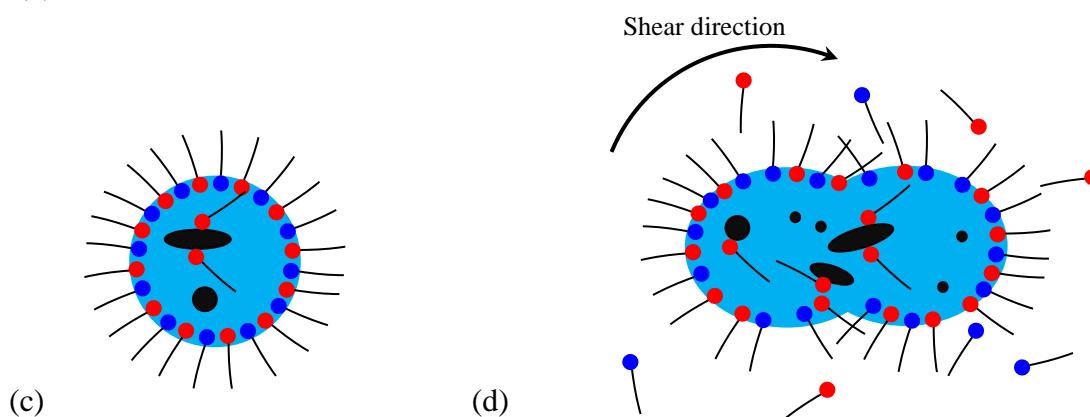
- Phase transformation of NPs from organic phase to aqueous phase was performed by the formation a double layer of stabilizers molecules (admicelles) around NPs. After modification of NPs functionalization, the hydrophilic head of stabilizer molecules were free inside the solution that results in switching of hydrophobic NPs to hydrophilic one [16]. The hydrodynamic average

size of NPs before and after phase transformation confirmed a formation of stabilizer admicelles around particles. The average hydrodynamic size of NPs was equal to 8.91 ± 0.39 nm and 13.8 ± 0.98 nm before and after phase transformation respectively. Around 4.9 nm increment in hydrodynamic size is an evidence for the formation of admicelles around the NPs. Fig. 4b and c illustrate the TEM images of NPs and mechanisms of rod shape appearance respectively. The TEM images disclose the conversion of spherical morphology to rod shape by increasing the temperature and reactants concentration. Attachment of stabilizer molecules on surface of primary nuclei and change of crystal facets growth rate (Fig. 4c) and stretched of spherical droplets of reverse microemulsion to ellipsoidal shape across the shear rate direction (Fig. 4c) are main reasons for rod shape morphology appearance [17]. Table 1 provide some more information about concentration and morphology of final iron oxide NPs.





(b)



(c)

(d)

Fig. 4. The procedure of preparation and functionalizing of iron oxide NPs, (b) effect of temperature and reactant concentration on morphology of iron oxide NPs (c, d) mechanisms of rod NPs appearance.

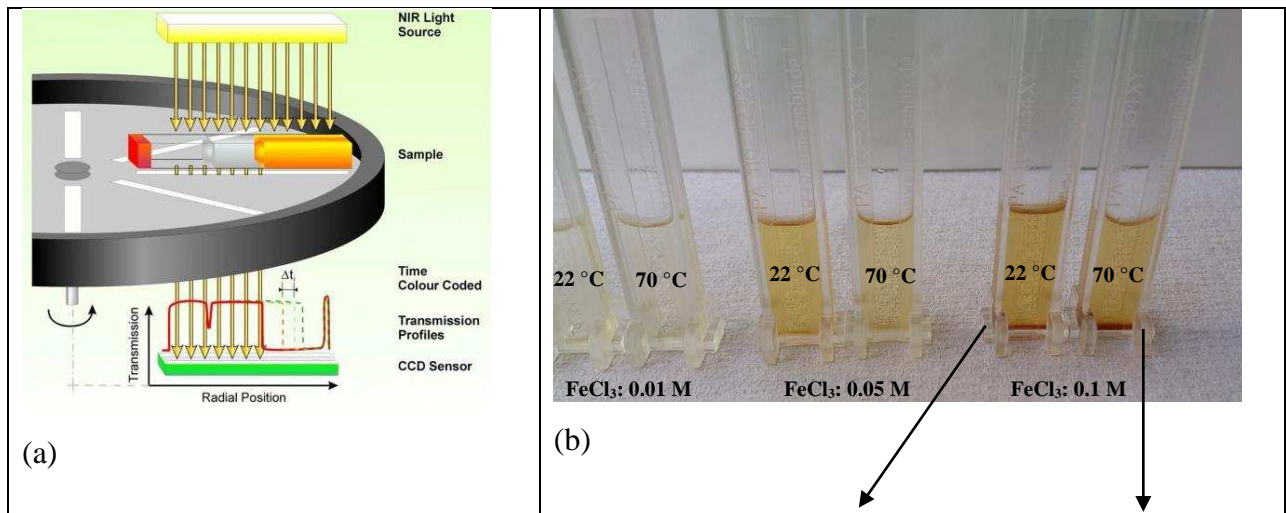
Table 1. The characterization of iron oxide nanoparticle at different conditions.

Reaction conditions	Morphology	Concentration measured by AAS (ppm)	TEM image processing		
			Average size	Polydispersity index	Aspect ratio of rod NPs
FeCl ₃ : 0.01 M Tem: 22 °C	Spherical	64	2.1	0.059	1
FeCl ₃ : 0.05 M Tem: 22 °C	Spherical	298	5.4	0.029	1
FeCl ₃ : 0.1 M Tem: 22 °C	Mix Spherical/Rod	594	8.5	0.161	-
FeCl ₃ : 0.01 M Tem: 70 °C	Mix Spherical/Rod	61	3.6	0.263	-

FeCl ₃ : 0.05 M Tem: 70 °C	Rod	321	7.3	0.042	2.66
FeCl ₃ : 0.1 M Tem: 70 °C	Rod	618	13.3	0.070	3.41

50 weight percent of LiBr was added to different iron oxide nanofluids to produce a binary nanofluid of LiBr. A dispersion analyzer (LUMiSizer 6110) instrument was used to determine the stability of binary nanofluids, Fig. 5a [17]. A near-infrared (NIR) light scan the sample during high speed centrifugation and the stability of binary nanofluids were determined based on final transmission pattern of NIR light. The binary nanofluids (0.5 ml) were filled in a polycarbonate capillary cell (Fig. 5b) and centrifuged for about 3 h (255 profile and 44 interval) at 3150 rpm (light factor 1, 25 °C, 870 nm NIR LED) which is equivalent to 6 months in real condition. The instability curves of different samples is shown in Fig. 5c.

The transmission curves of the binary nanofluids in Fig. 5d display a region of complete absorption, which indicates a polydisperse sedimentation pattern without observing any particle-particle attachment [19]. Moreover, the thin width regions of NIR transmission pattern imply high stability of samples for a long period of time. Fig. 5d also illustrates binary nanofluid samples and TEM photo of NPs (FeCl₃: 0.01 M, Tem=22 °C) after 6 month immobility that clearly verified the long shelf-life of binary nanofluids.



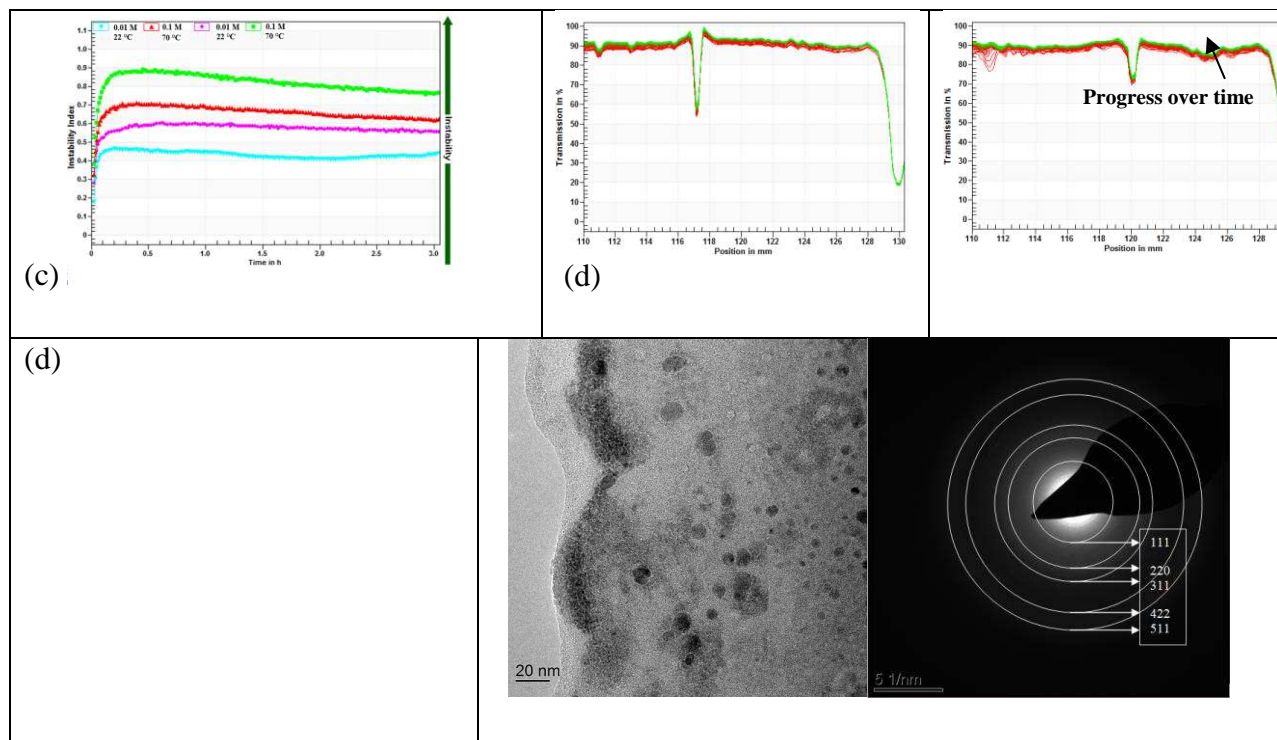


Fig. 5. (a) Schematic configuration of the analytical photo-centrifuge system LUMiSizer® [18], (b) polycarbonate capillary cell containing samples after centrifuge process (c) instability profile and (d) NIR transmission pattern of binary nanofluids, (e, f) binary nanofluid samples, TEM and SAED images of NPs (FeCl_3 : 0.01 M, $T_{em}=22\text{ }^\circ\text{C}$) after six month immobility.

3.2. Photo-thermal efficiency of binary nanofluid

Fig. 6 shows the UV-visible absorption spectra of the resulting nanofluids. The shift of UV spectra to right side is because of increasing concentration of NPs; however the change of morphology also affect on UV-visible adsorption spectra. The adsorption band of spectra shows the capability of nanofluids in the visible light spectrum, which is promising for potential photo-thermal conversion applications [33].

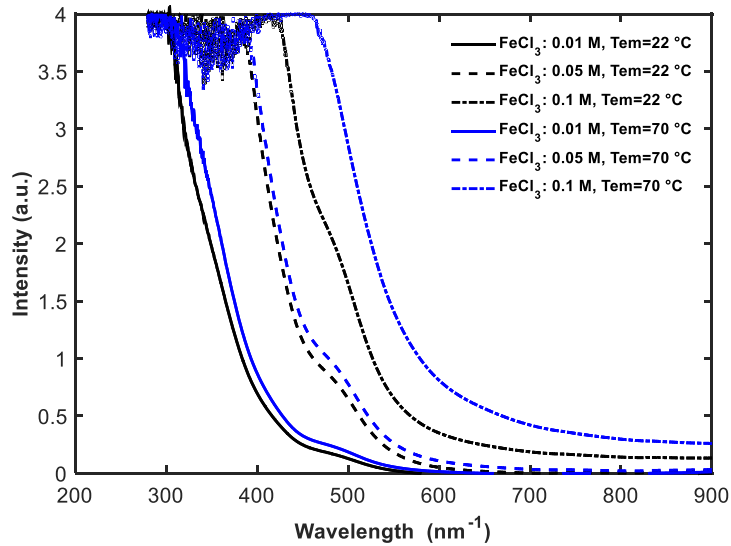


Fig. 6. UV-vis absorption spectra of Fe_3O_4 /water nanofluids with normalized absorbance.

Two nanofluids (FeCl_3 : 0.01, $T_{\text{em}}=22\text{ }^\circ\text{C}$ and FeCl_3 :0.05 M, $T_{\text{em}}=70\text{ }^\circ\text{C}$) were selected as representative of spherical and rod shape morphology for photo-thermal conversion evaluation. Fig. 7 illustrates the increasing of nanofluids bulk temperature and deionized water under solar radiative intensity of 10 sun ($\sim 10000\text{ W/m}^2$) for 40 minutes during which the temperature was recorded. After 40 minutes' illumination, the solar simulator was shut down and samples stayed for cooling down.

According to Fig. 7a, the temperature of deionized water increased slowly, and reached only $52\text{ }^\circ\text{C}$ after 40 minutes illumination. Only 0.73 g water was evaporated during 40 minutes, and the maximum evaporation rate reached only 0.46 mg/s. In the first 20 min, temperature inside the volume was non-uniform and the largest temperature difference was $5\text{ }^\circ\text{C}$. That is because the light intensity decreases along the optical depth, resulting in higher absorption at the surface. After then, temperature gradient shrink to less than $2\text{ }^\circ\text{C}$, indicating higher surface evaporation rate reduced the surface temperature increasing rate, leading a more uniform temperature profile.

Addition of iron oxide NPs into water improved the temperature increasing obviously. For iron oxide nanofluid with concentration of 321 mg/L, the highest temperature reached $66\text{ }^\circ\text{C}$ after 40 minutes illumination that is 21 percent higher than pure water. For all nanofluids, the

surface temperature was higher and mean temperature was more non-uniform compared to pure water. The non-uniformity of temperature were proportional to NPs concentration.

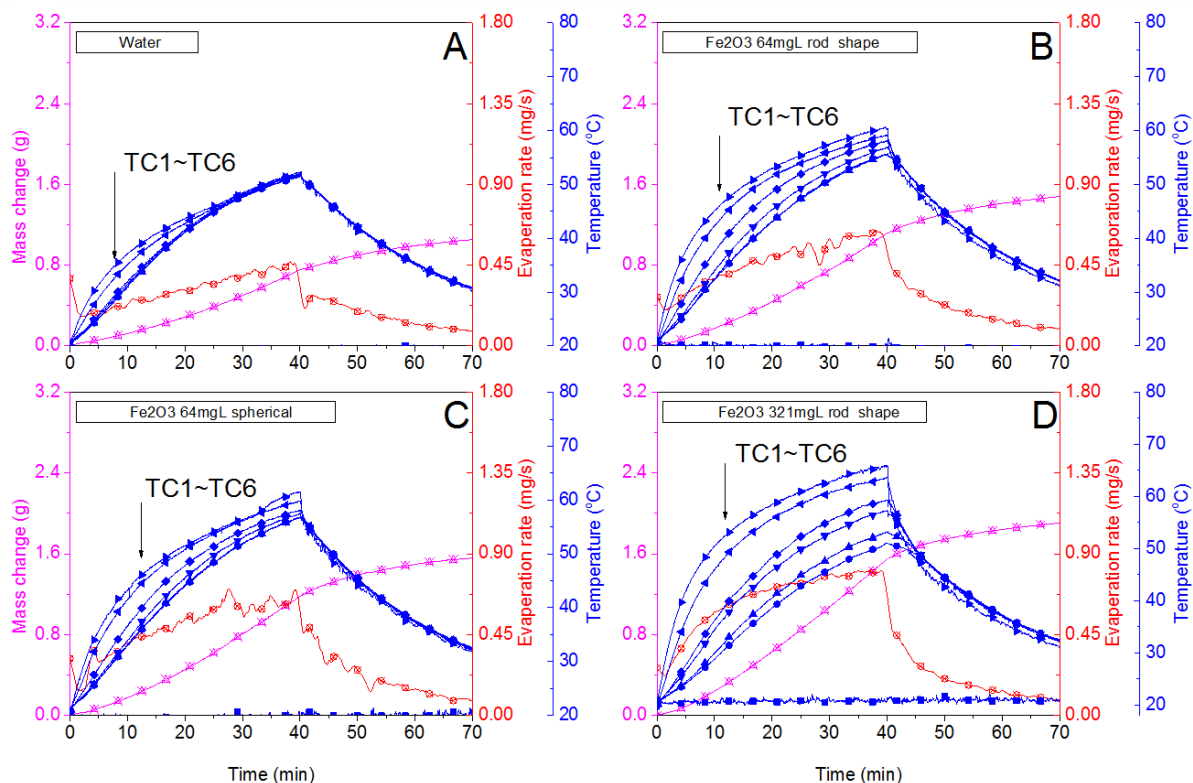


Fig. 7. Comparison of increasing temperature of thermocouples, mass change, evaporation rate of binary nanofluid and deionized water under 10 sun illumination: a) deionized water, b) 64 mg rod shape, c) 64 mg spherical shape, d) 321 mg rod shape.

The surface and bottom temperature of samples are more clearly illustrated in Fig. 8. According to Fig. 8, the highest temperature (TC6) was elevated comparing to pure water while the lowest temperature was decreased when the concentration of NPs increased. For instance, TC1=55.7 °C at t=40 min for 64 mg/L concentration of rod shape NPs, while TC1=50.5 °C at 321 mg/L. A higher concentration of NPs led to a high non-uniform temperature distribution and more energy is concentrated on the surface, producing a localized heat at the surface that is beneficial for steam evaporation

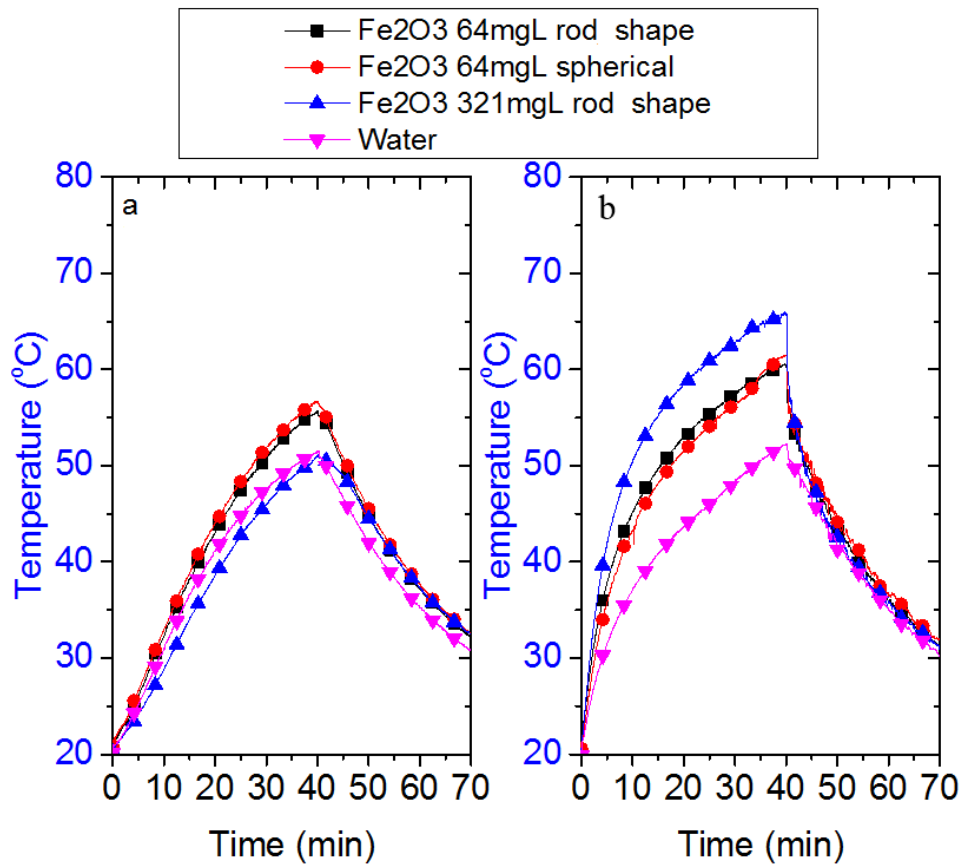


Fig. 8. a) Bottom temperature (TC1) and b) surface temperature (TC6) of different binary nanofluids with time under both 10 sun.

Evaporated mass change and evaporation rate also were significantly increased for binary nanofluid compared to pure water. The highest evaporation rate raised to 0.80 mg/s for 321 mg/L NPs rod shape concentration, almost twice of that of deionized water (0.46 mg/s). According to radiative heat transfer process [20] (Modest, 2003) more solar radiative energy will be converted to thermal form when the concentration of NPs is increased.

As mentioned before, the lower bulk temperature was observed for higher concentration of NPs that indicating less sensible heat at higher concentration of NPs. The sensible heat and latent heat (energy consumed to evaporate water) have been calculated and illustrated in Fig.9 in order to estimate the consumption energy (energy consumed to heat up the bulk).

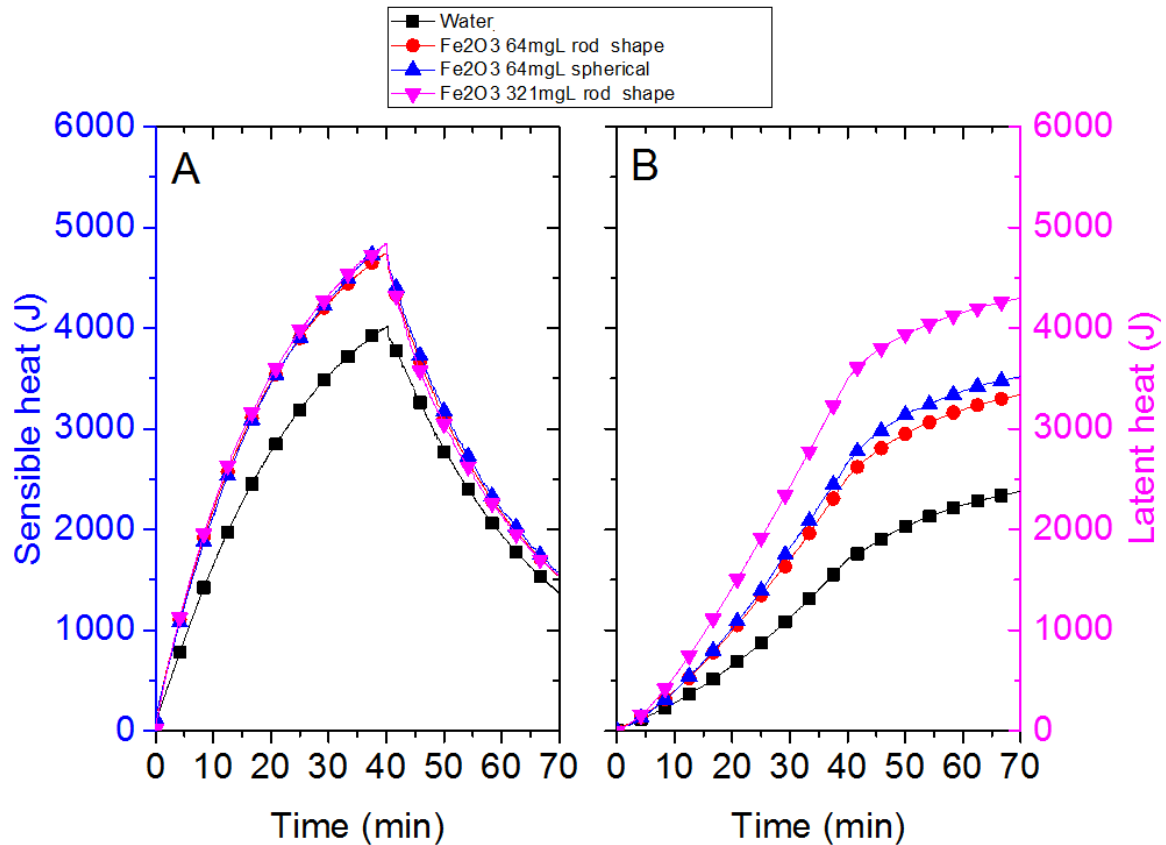


Fig. 9. a) Sensible heat and b) latent heat of different concentrations with time under 10 sun.

The latent heat reached 3800 J after 40 minutes illumination for 321 mg/L rod shape NPs, but for water, it is less than 2000 J under the same condition at same time, which means NPs absorbed more radiative energy and convert it to the latent form to evaporate water. In order to investigate the energy conversion efficiency, percentage of sensible heat and latent heat under 10 sun are presented in Fig. 10.

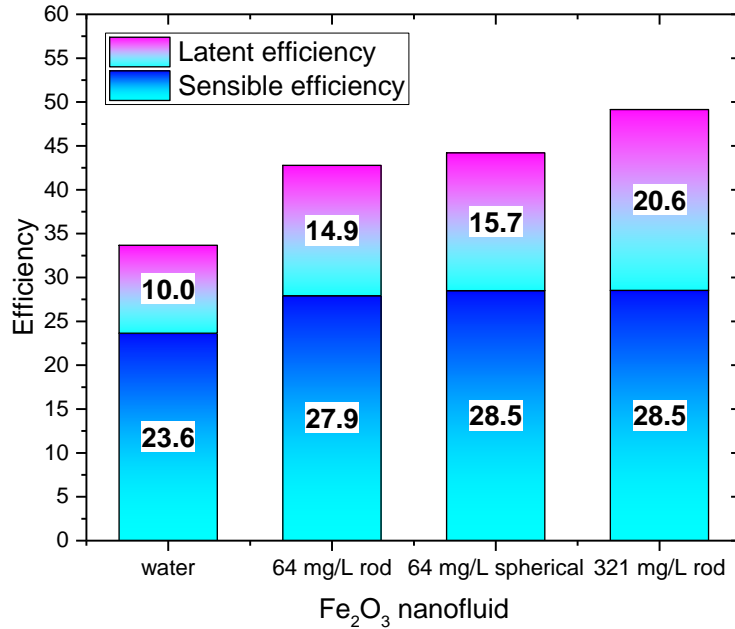


Fig. 10. Energy efficiency calculated from converted latent and sensible heat.

Fig. 10 clearly shows that iron oxide NPs increased the total energy absorption of solar radiative energy. For example, total efficiency for pure water is 33.6%, but it is 44.2% for 64 mg/L spherical NPs. Increasing of NPs concentration will slightly increase energy conversion efficiency, which is in agreement with results of other research [21, 22]. Increasing concentration will increase latent heat efficiency significantly but increase sensible heat efficiency slightly. This means the increasing concentration of NPs will absorb more solar energy and allocate more absorbed energy to evaporate water. The purpose of adding NPs into solar receiver is not only to increase photon trapping efficiency, but also to evaporate more water under lower bulk temperature.

Conclusions

In recent years, solar air conditioning has applied as green and environment friendly system for temperature, humidity and distribution of air controlling. In this study, a high stable binary iron

oxide nanofluid (50 wt% LiBr) was synthesized for the application in solar absorption air conditioning.

- Uniform spherical and rod shape NPs were produced by reverse microemulsion method. The particles obtained with lower concentration were small, spherical and monodispersed while the nanoparticles were converted to rod shape by increasing concentration.
- xx is used to engineer the stability of the nanofluid. The stability analysis of nanoparticles in the presence of 50 wt. % of lithium bromide showed the the formed nanofluid can be stable for a long period of xx months.
- The analysis of bulk temperature increase and surface evaporation rate of iron oxide based nanofluids under solar simulator highlights the efficient photo-to-thermal energy conversion and the consequently enhanced vaporizing ability.
- Both sensible heat and latent heat capture were boosted for nanofluid while the rate of latent heat increasing was higher than sensible heat by increasing NPs concentration.
- Superior stability of binary nanofluid against agglomeration and proper photo-to-thermal energy conversion efficacy support the use of proposed novel binary nanofluid in solar vapor adsorption refrigeration systems.

References

- [1] Dossat R. J., T. J. Horan, Principles of Refrigeration Paperback, Prentice Hall; 5 edition, ISBN: 0130272701, 2001.
- [2] Elsafty, A., Solar Air Conditioning System: Water/Lithium Bromide Vapour Absorption system Perfect Paperback, Lap Lambert Academic Publishing, 2013.
- [3] H. Kim, J. Jeong, Y. Tae, Heat and mass transfer enhancement for falling film absorption process by SiO₂ binary nanofluids, Int. J. Refrig. 35 (2012) 645-651.

- [4] J.Y. Jung, E.S. Kim, Y. Nam, Y.T. Kang, The study on the critical heat flux and pool boiling heat transfer coefficient of binary nanofluids ($\text{H}_2\text{O}/\text{LiBr} + \text{Al}_2\text{O}_3$), *Int. J. Refrig.* 36 (2013) 1056-1061.
- [5] O. Neumann, A. S. Urban, J. Day, Surbhi Lal, P. Nordlander, N. J. Halas, Solar Vapor Generation Enabled by Nanoparticles, *ACS Nano*, 7 (2013) 42-49.
- [6] Q. Jiang, W. Zeng, C. Zhang, Z. Meng, J. Wu, Q. Zhu, D. Wu, H. Zhu, Broadband absorption and enhanced photothermal conversion property of octopod-like $\text{Ag}@\text{Ag}_2\text{S}$ core@shell structures with gradually varying shell thickness, *Scientific Reports*, 7 (2017) 17782.
- [7] S. Khashan, S. Dagher, S. Al Omari, N. Tit, E. Elnajjar, B. Mathew, A. Hilal-Alnaqbi, Photo-thermal characteristics of water-based $\text{Fe}_3\text{O}_4@\text{SiO}_2$ nanofluid for solar-thermal applications, *Mater. Res. Express* 4 (2017) 055701.
- [8] S.C. Alfaro, S. Lafon, J.L. Rajot, P. Formenti, A. Gaudichet, Iron oxides and light absorption by pure desert dust: An experimental study, *J. Geophys. Res.* 109 (2004) 1-9.
- [9] D. Wu, H. Zhu, L. Wang, L. Liua, Critical issues in nanofluids preparation, characterization and thermal conductivity, *Curr. Nano. sci.* 5 (2009) 103-112.
- [10] Malik, M.A., M. Y. Wani, M. A. Hashim, Microemulsion method: A novel route to synthesize organic and inorganic nanomaterials, *Arabian Journal of Chemistry*, 5 (2012) 397-417.
- [11] Rees, G. D., R. Evans Gowing, S. J. Hammond, B. H. Robinson, Formation and Morphology of Calcium Sulfate Nanoparticles and Nanowires in Water-in-Oil Microemulsions, *Langmuir*, 15 (1999) 1993-2002.
- [12] J. Vidal-Vidal, J. Rivasb, M.A. Lopez-Quintelaa, Synthesis of monodisperse maghemite nanoparticles by the microemulsion method, *Colloids and Surfaces A: Physicochemical and Engineering Aspects*, 288 (2006) 44-51.
- [13] L.H. Han, H. Liu, Y. Wei, In situ synthesis of hematite nanoparticles using a low-temperature microemulsion method, *Powder Technology*, 207 (2011) 42-46.

- [14] R. Massart, Preparation of aqueous magnetic liquids in alkaline and acidic media, *IEEE Trans Magn.* 17(1981) 1247-1248.
- [15] E. Nourafkana, H. Gao, Z. Hu, D. Wen, Formulation optimization of reverse microemulsions using design of experiments for nanoparticles synthesis, *Chemical Engineering Research and Design*, 125 (2017) 367-384.
- [16] R.A. Sperling, W.J. Parak, A Review: Surface modification, functionalization and bio conjugation of colloidal inorganic nanoparticles, *Phil. Trans. R. Soc. A.* 368 (2010) 1333-1383.
- [17] X. Li, W. Zheng, G. He, R. Zhao, D. Liu, Morphology Control of TiO₂ Nanoparticle in Microemulsion and Its Photocatalytic Property, *ACS Sustainable Chem. Eng.* 2 (2014) 288-295.
- [18] J. Gross-Rother, N. Herrmann, M. Blech, S.R. Pinnapireddy, P. Garidel, U. Bakowsky, The application of STEP-technology® for particle and protein dispersion detection studies in biopharmaceutical research, *International Journal of Pharmaceutics*, 543 (2018) 257-268.
- [19] B. Schluter, R. Mulhaupt, A. Kailer, Synthesis and Tribological Characterization of Stable Dispersions of Thermally Reduced Graphite Oxide, *Tribol. Lett.* 53 (2014) 353-363.
- [20] Modest, M.F., *Radiative Heat Transfer*, Second Edition, Academic Press, 2003.
- [21] E.P. Bandarra Filho, O.S.H. Mendoza, C.L.L. Beicker, A. Menezes, D. Wen, Experimental investigation of a silver nanoparticle-based direct absorption solar thermal system, *Energy Convers. Manag.* 84 (2014) 261-267.
- [22] A. Zeiny, H. Jin, L. Bai, G. Lin, D. Wen, A comparative study of direct absorption nanofluids for solar thermal applications, *Solar Energy*, 161 (2018) 74-82.